Sex-specific effect of prenatal alcohol exposure on N-Methyl-D-Aspartate Receptor function in orbitofrontal cortex pyramidal neurons of mice

Valentina Licheri[1], **Jayapriya Chandrasekaran**[1], **Clark W. Bird**[1], **C. Fernando Valenzuela**[1,2], **Jonathan L. Brigman**[1,2,*]

[1]Department of Neurosciences, University of New Mexico School of Medicine, Albuquerque NM, USA

[2]New Mexico Alcohol Research Center, UNM Health Sciences Center, Albuquerque NM, USA.

Abstract

Background: Alcohol consumption during pregnancy can produce behavioral and cognitive deficits that persist into adulthood including impairments in executive functions, learning, planning and cognitive flexibility. We have previously shown that moderate prenatal alcohol exposure (PAE) significantly impairs reversal learning, a measure of flexibility mediated across species by different brain areas including the orbital frontal cortex (OFC). Reversal learning is likewise impaired by genetic or pharmacological inactivation of GluN2B subunit-containing N-Methyl-D-aspartate receptors (NMDARs). In the current study, we tested the hypothesis that moderate PAE persistently alters the number and function of GluN2B subunit-containing NMDARs in OFC pyramidal neurons of adult mice.

Methods: We used a rodent model of FASD and left offspring undisturbed until adulthood. Using whole-cell patch-clamp recordings we assessed NMDAR function in slices from 90–100-day-old male and female PAE, and control mice. Pharmacologically-isolated NMDA receptor-mediated evoked excitatory post-synaptic currents (NMDA-eEPSCs) were recorded in the absence and presence of the GluN2B antagonist, Ro25–6981(1 μM). In a subset of littermates, the level of GluN2B protein expression in the synaptic fraction was evaluated using western blotting technique.

Results: Our results indicate that PAE females show significantly larger (~23%) NMDA-eEPSC amplitude than controls, while PAE induced a significant decrease (~ 17%) in NMDA-eEPSC current density of pyramidal neurons recorded in slices coming from male mice. NMDA eEPSC decay time was not affected in PAE-exposed mice from either sex. The contribution of GluN2B subunit-containing NMDARs to the eEPSCs was not significantly altered by PAE. Moreover, there were no significant changes in protein expression in the synaptic fraction of PAE males and females.

[*]Correspondence to: Jonathan L. Brigman, PhD, Department of Neurosciences, University of New Mexico School of Medicine, MSC08 4740, 1 University of New Mexico, Albuquerque, NM, USA 87131-0001, jbrigman@salud.unm.edu, Telephone: 505-272-2868, Fax: 505-272-8082.

Conclusions: These findings suggest that low-to-moderate PAE modulates NMDAR function in pyramidal neurons in a sex specific manner, although we did not find evidence that this is mediated by dysfunction of synaptic GluN2B subunit-containing NMDARs.

Keywords

Prenatal Alcohol exposure; NMDA receptors-subunits; OFC; pyramidal neurons; linear mixed model; synaptic fraction

Introduction

Alcohol consumption during pregnancy is a serious public health concern. In fact, several studies report that more than one in nine pregnant women drink alcohol regularly in the United State, (May et al., 2009; Tan et al., 2015; Fontaine et al., 2016; Popova et al., 2017; Pfinder and Lhachimi, 2020) while in Europe almost 16% of women consume alcohol during pregnancy (Mårdby et al., 2017). Drinking during this critical period is well established to have a long-lasting negative impact on the development of offspring, including lifelong physical, behavioral and cognitive deficits. Collectively, these impairments are referred to as Fetal Alcohol Spectrum Disorders (FASD) (Ehrhart et al., 2019). Meta-analysis studies reported that rates of FASD exceed 1% in 76 countries (Lange et al., 2017) and between 2–5% in the United States (May et al., 2009; May et al., 2014). Given these estimates, understanding the mechanisms by which alcohol leads to life-long alterations in brain function is a critical public health issue.

Studies in humans have found that moderate Prenatal Alcohol Exposure (PAE) is associated with cognitive (Burden et al., 2005a; Burden et al., 2005b), and behavioral deficits during adolescence (Pfinder and Lhachimi, 2020) and adulthood (Day et al., 2013; Lynch et al., 2015). Rodent investigations have demonstrated that binge-like ethanol exposure during the equivalent to the third trimester of human pregnancy is sufficient to induce cell death in the cerebral cortex (Olney, 2004; Saito et al., 2007; Wilson and Cudd, 2011). We previously demonstrated that moderate PAE significantly increases maladaptive perseveration during reversal learning (Marquardt et al., 2014). PAE was also shown to significantly alter both single unit and local field potential (LFP) activity in the orbitofrontal cortex (OFC) and in the dorsal striatum (DS) (Marquardt et al., 2020).

Recently, we have found that PAE increases the amplitude of spontaneous inhibitory post-synaptic currents (sIPSCs) in pyramidal neurons and alters GABAergic inter-neuronal numbers in OFC (Kenton et al., 2020). Alcohol is well known to affect not only GABAergic function, but also glutamatergic transmission in cortex (Carpenter-Hyland et al., 2004; Thomas et al., 2004; Skorput and Yeh, 2016). Studies have also found that N-Methyl-D-Aspartate receptors (NMDARs) play a critical role in several aspects of learning and behavioral flexibility in rodent models (Dong et al., 2013; Clark et al., 2017; Marquardt et al., 2019).

NMDARs are composed by two obligatory GluN1 subunits and two modulatory GluN2 or GluN3 subunits (Paoletti, 2011; Shipton and Paulsen, 2014). Glutamate binds to the GluN2 subunits, and four distinct isoforms of this subunit exist (A-D) (Laube et al., 1997; Anson

et al., 1998). In rodent brain, the GluN2A subunit starts its expression in hippocampus and cerebellum, and after birth gradually reaches whole brain in adulthood. Whereas the GluN2B-containing isoform is expressed from embryonic day (E)14 and continues to increase until postnatal day (P)7–10. After this period, this subunit is expressed only in the cerebral cortex, hippocampus, striatum and olfactory bulb (Cull-Candy et al., 2001; Paoletti et al., 2013). Importantly, hippocampal GluN2B has been shown to be reduced by PAE in mouse models (Samudio-Ruiz et al., 2010; Brady et al., 2013). Additionally, genetic or pharmacological loss of GluN2B function in the cortex produces analogous deficits in reversal learning as those observed in PAE mice (Brigman et al., 2013), also alters OFC pyramidal neuron firing and coherence, and aberrantly increases OFC-striatal synchrony (Marquardt et al., 2019). In the current study, we hypothesized that PAE reduces the function of GluN2B-containing NMDARs in OFC pyramidal neurons. To test this hypothesis, we evaluated the effects of a moderate PAE treatment on NMDAR-mediated synaptic currents in OFC pyramidal neurons in the absence and presence of Ro25–6981, a selective GluN2B antagonist, and measured protein expression levels of GluN2B subunit via western blotting.

Materials and Methods

All experimental procedures were performed in accordance with the National Institutes of Health Guide for Care and Use of Laboratory Animals and were approved by the University of New Mexico Health Sciences Center Institutional Animal Care and Use Committee.

Prenatal Alcohol Exposure Paradigm

PAE and control mice used for the current study were provided by the New Mexico Alcohol Research Center utilizing a model previously shown not to alter dam-pup interactions or lead to gross morphological changes in offspring (Brady et al., 2012; Marquardt et al., 2014). Briefly, female C57BL/6J mice PND 60 days (Jackson Laboratory, Bar Harbor, ME) were exposed to 0.066% (w/v) saccharin (SAC) (Sigma, product #S6047) or to Ethanol (EtOH) (KOPTEC, product #V1101) solution (5% w/v for 4 days, then 10% w/v) sweetened with 0.066% (w/v) saccharin for 4 hours per day (from 10:00 to 14:00 hours) during the dark cycle. After 1 week of drinking SAC or 10% EtOH solutions, individual females were placed into the cage of a singly housed male (Jackson Laboratory, Bar Harbor, ME) for 2 hours immediately following the drinking period (from 14:00 to 16:00 hours) for 5 days. Females continued the exposure to SAC and EtOH solutions throughout the 5-days mating period. Pregnancy was determined by monitoring weight gain every 3 to 4 days. Within 1 day of birth, the SAC and EtOH concentrations were halved every 2 days. The average of EtOH drinking consumption was 3.91 ± 0.18 g EtOH/kg/4 hours. SAC and PAE offspring were weaned ~PND 23. Offspring were housed in groups of 2–4 per cage at constant temperature and a relative humidity under reverse 12 hr light/dark (lights off 08:00 hr) with free access to water and standard laboratory food at all times. 77 mice (21 SAC males, 19 PAE males, 19 SAC females and 18 PAE females) from 48 litters (27 SAC and 21 PAE) were used to perform this study. Investigators were blind to the treatment group assignment.

Western blotting for protein expression

SAC and PAE male and female mice were used to quantify the expression of NMDAR subunits in the OFC. At 90 days of age, 20 mice per sex/exposure were anesthetized with isoflurane (Piramal Enterprises Limited, Telangana, India), then brains were extracted and snap frozen using 2-methyl butane (Avantar performance Materials, LLC, PA, USA). 2 mm diameter × 1 mm thickness micro-punches were taken from the OFC and frozen immediately on dry ice. In order to obtain sufficient membrane fraction for immunoblotting, micro punches from 4 brains were pooled resulting in n of 5/sex/exposure. Subcellular fractionation was performed as previously described (Goebel-Goody et al., 2009) to isolate the synaptic membrane fraction bound to post synaptic density. Briefly, tissue was homogenized with the Biomasher (VWR) in the homogenization buffer (Tris, pH 7.4, Ethylenediaminetetraacetic acid (EDTA), Ethylene glycol-bis(2-aminoethylether)-N,N,N', N'-tetraacetic acid (EGTA), sucrose, sodium fluoride, sodium orthovanadate, sodium pyrophosphate, β-glycerophosphate) (Sigma, St. Louis, MO) and protease inhibitor cocktail (Sigma, St. Louis, MO), then centrifuged twice (1000xg for 10 minutes at 4°C) to remove the nuclear debris. The resulting supernatant was centrifuged again (15,000xg for 30 minutes at 4°C) to isolate the crude synaptic and extra synaptic membrane. Hypo osmotic lysis was then done by treating the crude membrane fraction with ice cold water containing protease inhibitor cocktail (Sigma, St. Louis, MO). Following which the crude membrane fraction was sonicated and treated with HEPES NaOH buffer (PH 7.4), (Sigma, St. Louis, MO) for 30 minutes on ice. Centrifugation (15,000xg for 30 minutes at 4°C) resulted in lysate pellet and lysate supernatant containing the enriched synaptosomal membrane fraction. The lysate pellet upon treatment with Triton-X100 buffer (Tris, pH 7.4, NaF, EDTA, EGTA, sodium orthovanadate, and protease inhibitor cocktail) and centrifugation (15,000xg for 30 minutes at 4°C) yielded the synaptic membrane fraction bound to the post synaptic density (Triton-insoluble particulate, TxP) and extra-synaptic (Triton-soluble, TxS) membrane fraction. Subsequent protein quantification was performed on the TxP fraction. Protein concentration was determined by the fluorescence-based quantification using the Qubit fluorometric quantification system (Invitrogen Qubit 4 fluorometer). NMDAR subunit (GluN2B, GluN1) levels in the synaptic membrane fraction bound to post-synaptic density were determined using immunoblotting. The samples were diluted in 4x sample buffer (Thermo Fisher Scientific, catalog number: NP0007). Equal protein quantity (5μg) was loaded onto 4–12% Bis Tris gel (Thermo Fisher Scientific, catalog number: NP0336) and ran at 165volts for 1 hr 10 minutes to separate the proteins. The transfer of proteins to the Immobilon PVDF Transfer Membrane (Sigma, MO catalog number: IPFL0780) was performed at 40volts for 1 hour 20 minutes. The membrane was blocked in LICOR blocking buffer (LI-COR; catalog number: 927–40000) for an hour following which incubation with the primary antibodies- anti-GluN2B (1:750, Cell Signaling; catalog number: 4212S), anti-GluN1 (1:1500, Cell Signaling, catalog number: 5704S) was done overnight at 4°C. Following day, the membrane was incubated in secondary antibody-goat anti-rabbit IRDye 680RD (infra-red fluorescence-based secondary antibody, LI-COR, catalog number: 926–68071) for 45 minutes. Immuno-reactivity was detected by scanning with LI-COR Odyssey imager (Serial number: ODY-1518, LI-COR, Nebraska, USA) and analyzed using Li-COR Image lite software (LI-COR, Nebraska, USA). Each protein of

interest was normalized to total protein which was obtained by Coomassie staining (Sigma, MO, catalog number: 42660).

Brain slice preparation

Brain slices containing the OFC were prepared from adult offspring SAC and PAE mice (97.64 ± 1.09 days of age). Mice were deeply anesthetized with ketamine (25 mg/kg intraperitoneal) and intra-cardiac perfused with cold cutting solution containing in (mM): 92 N-methyl-D-glucamine (NMDG), 2.5 KCl, 10 $MgSO_4$, 0.5 $CaCl_2$, 1.25 NaH_2PO_4, 30 $NaHCO_3$, 20 Hepes, 25 Glucose, 2 Thiourea, 3 Na-Pyruvate, 5 Na-ascorbate (pH to 7.3–7.4 with HCl and bubbled with 95% O_2 /5% CO_2, adjusted osmolarity to 290–310 mOsm). The brain was rapidly removed from the skull and transferred for 2 min into ice-cold cutting solution. Coronal slices (300 μm thick) were cut with a Leica VT1000 plus vibratome (Leica Microsystems, Bannockburn, IL), transferred to an incubation chamber held at 34 °C and containing NMDG cutting solution to which increasing amounts of 2M NaCl (dissolved in NMDG cutting solution) were added in a step-wise fashion (250 μl at 0 min, 250 μl at 5 min, 500 μl at 10 min, 1 ml at 15 min, and 2 ml at 20 min) until a final concentration of 52 mM was reached. Slices recovered in a holding chamber (model BSC-PC, Warner Instruments, Hamden, CT) with artificial cerebral spinal fluid (aCSF) containing in (mM): 92 NaCl, 2.5 KCl, 1.25 NaH_2PO_4, 30 $NaHCO_3$, 25 glucose, 20 HEPES, 2 Thiourea, 3 Na-Pyruvate, 5 Na-ascorbate, 2 $CaCl_2$, and 1 $MgSO_4$. (pH to 7.3–7.4 with a few drops of 1 M NaOH,) bubbled with 95% O_2/ 5% CO_2, (290–310 mOsm). Slices were then kept at room temperature for a least 40–60 min before the start of electrophysiological recordings.

Whole-cell recordings

After incubation, a hemi-slice was placed in a recording chamber with slice support (Cat # RC-27L; Warner Instruments) to allow flow of aCSF above and below the slice. The recordings were performed in presence of aCSF containing in (mM): 126 NaCl, 3 KCl, 1.25 NaH2PO4, 1 $MgSO_4$, 2 $CaCl_2$, 26 $NaHCO_3$, 10 glucose, 5 Na-ascorbate, osmolarity 290–310 mOsm, pH 7.4 bubbled with 95% O_2 / 5% CO_2 and delivered to the chamber at a flow rate of 2 ml/min using a peristaltic pump (Master Flex, model 7518–10, Cole-Parmer, Vernon Hills, IL). Temperature was maintained at 34 °C with a dual automatic temperature controller (Model TC-344B) that was also connected to an in-line solution heater (Model SH-27B) (Warner instruments).

Pyramidal neurons in lateral OFC were identified using an Olympus BX50WI upright microscope (Olympus, Center Valley, PA) equipped with infra-red differential interference contrast optics connected to a charge-coupled device camera (CCD100, DAGE-MTI, Michigan City, IN). Recording pipettes were prepared from filament-containing borosilicate capillary glass (outside diameter, 1.5 mm, inside diameter 0.86 mm, catalog # BF150-86-10; Sutter Instruments) and pulled to a resistance between 2.5 and 5.0 MΩ using a DMZ Universal Electrode Puller (Zeitz-Instruments Vertriebs GmbH, Martinsried, Germany).

The internal pipette solution contained (in mM): 120 CsCl, 10 Hepes, 2 MgCl2, 1 EGTA, 2 MgATP, 0.3 mM NaGTP, 1 QX314, adjusted to 288 mOsm, pH 7.3–7.4 was used to record electrically-evoked excitatory postsynaptic currents (eEPSCs) (Badanich

et al. 2013). A concentric bipolar stimulating electrode (FHC, USA) was placed in proximity to the recorded cell. Stimulus pulses were delivered every 20 sec to elicit a stable and submaximal evoked (approx. 50% maximum amplitude) response with a Master-8 pulse stimulator connected to a stimulus isolator (ISO-Flex, AMPI, Jerusalem, Israel). NMDA-eEPSCs were evoked at a holding potential of +40 mV and in presence of picrotoxin (100 μM, Hello Bio) and AMPAR antagonist 2,3-dioxo-6-nitro-1,2,3,4-tetrahydrobenzo[*f*]quinoxaline-7-sulfonamide (NBQX 10 μM, Hello Bio). NMDA/GluN2B mediated currents were blocked using Ro25–6981 (1 μM). At the end of each recording, NMDA-eEPSCs were blocked with the non-selective NMDAR-antagonist D.L-APV (50 μM, Hello Bio).

After initiation of the whole-cell recording, stable responses of NMDA-eEPSCs were observed over 5–15 min. We started the recording baseline for 5 min, subsequently the selective blocker of GluN2B was perfused for 15 min. DL-APV was applied at the end for 10 min. The NMDA-eEPSCs mediated by GluN2B subunit-containing receptors were analysed during the last 5 minutes of bath-application and normalized to the baseline period.

Whole-cell recordings were conducted with an Axopatch 200-B amplifier (Molecular Devices, Sunnyvale, CA). Currents were filtered at at 2 kHz, and digitized at 5 kHz using an analog-to -digital signal converter Model 1440A (Molecular Devices, Sunnyvale, CA). Data were acquired using Clampex software version 10.7 (Molecular Devices, Sunnyvale, CA). Only recordings with a stable access resistance that varied < 25% and did not exceed 30 MΩ were included in the analysis. Off-line analysis was performed using Clampfit 10.7 (Molecular Devices, Sunnyvale, CA). The eEPSCs amplitude was measured from the baseline to the peak of response. The current density was calculated by dividing the amplitude by the capacitance (pA/pF), while the decay time was estimated by curve fitting with a single exponential function. Clampfit statistics function was used to measure the total charge of eEPSCs (area under the curve, pA*ms) for the baseline and Ro25–6981 conditions. Since, the aim of the present study was to characterize the possible effects mediated by PAE on NMDA currents in OFC pyramidal neurons, only cells showing membrane capacitances greater than 100 pF (which most likely correspond to pyramidal neurons) were included in the analysis (Kenton et al., 2020, Badanich et al., 2013).

Drugs

All reagents and drugs used in the current study unless otherwise indicated were purchased from Sigma (Sigma-Aldrich). Most drugs were hydrochloride salts and were dissolved in MilliQ water to make stock solutions. Picrotoxin was dissolved in methyl sulfoxide (DMSO) (Thermo-Fisher Scientific) >99.9%, as stock solution, and after dilution, DMSO concentration was less than 0.1%. The stock solutions were stored frozen in aliquots, and before each single recording they were diluted in ACSF to their final concentrations.

Statistical analysis

Statistical analyses were performed using Prism version 9.0.1 (GraphPad Software, San Diego, CA) and SPSS version 26 (IBM, Armonk, NY). Power analysis (significance criterion at $\alpha = 0.05$ and statistical power at 80%) determined that 16 animals were required

to detect group differences. Rout test 1% was used to detect possible outliers, and 22 values were removed prior to analysis. Data are expressed as means ± SEM (please see Table 1). For electrophysiology data, we recorded multiple cells from several mice and from several litters, then in order to control intra-litter effect we performed a Linear Mixed Model (LMM) analysis using SPSS software (Golub and Sobin, 2020). The model was built in a step-wise fashion using method adopted from Linear Mixed Models: A Practical Guide Using Statistical Software book (West et al., 2007). We used the following procedure for each variable analysed (please see Table 2). In the first step, a LMM including the litter random effect associated with intercept and using homogeneous residual error variances between experimental groups was built, while in a second LMM we excluded the litter random effect. Then, we used the −2-log restricted maximum likelihood value for each model to perform a likelihood ratio chi-square test. If the p-value for the last test was < 0.05, we included the random effects in subsequent model. While, if the p-value was > 0.05, we excluded the litter effect from the final model.

Next, we built a model to test the appropriateness of inclusion or exclusion of heterogeneous residual error variances for experimental groups. Then, we performed another likelihood ratio chi-square test. If the test showed a p-value < 0.05, in the next model heterogeneous residual error variances were included. Table 2 reports F-ratios (calculated using Satterthwaite approximated degrees of freedom) and p-values for Type III F-tests for sex, exposure and interaction between fixed factors from the final LMM for each variable analysed.

The effect sizes for sex and exposure were calculated using Hedges' g formula. The normality of residuals was calculated using Shapiro-Wilkes test, and if p- value < 0.05 the residuals violated assumptions of normality. In this case, although the normality of residuals does not affect parameter estimates in multilevel models (Gelman and Hill, 2007) we performed non-parametric Mann-Whitney U test for fixed effects sex and exposure including effect size as $r = \frac{Z}{\sqrt{N}}$, where Z is Standard statistic, and N is the total of measurements. Mann-Whitney U results were reported in Table 2, and the variables that passed Shapiro-Wilkes test are amplitude and decay time measured after Ro25–6981 bath-application. For the western blot data, two-way repeated measures ANOVA with multiple comparison. All data presented are mean ± standard error of the mean (SEM).

Results

PAE effects on NMDA receptor-mediated evoked EPSCs

To evaluate if prenatal alcohol exposure alters the activity of NMDARs in OFC pyramidal neurons, evoked NMDA-eEPSCs were recorded in slices. Cell membrane capacitance did not show significant differences between controls and PAE in all experimental groups (LMMs: sex: $F_{(1,180)} = 2.127$, p= 0.147, Hedges's g = 0.2042; exposure effect: $F_{(1,180)} = 0.831$, p = 0.363, Hedges's g = 0.1342; sex*exposure effect: $F_{(1,180)} = 1.876$, p = 0.172,) (Fig 1A). The random effect of litter did not significantly improve LMM for capacitance and was not included in the final model. The analysis of membrane resistance indicated a sex significant effect (LMMs: sex: $F_{(1,179)} = 5.662$, p = 0.018, Hedges's g = 0.3383), no

effect of exposure (LMMs: exposure: $F(1,179) = 0.119$, $p = 0.730$, Hedges's $g = 0.0478$) and no sex*exposure effect (LMMs: sex*exposure: $F(1,179) = 1.713$, $p = 0.192$ (Fig 1B). Random effect of litter on membrane resistance was not included in the final LMM, because the p value of the likelihood ratio test was >0.05. For analysis of NMDA-eEPSCs amplitude, the likelihood ratio test indicated to not include the litter effect as a random effect, and the LMMs revealed that exposure did not modulate the amplitude (LMMs: exposure: $F(1,171) = 0.535$, $p = 0.466$, Hedges's $g = 0.1336$). Moreover the analysis indicated no significant effect of sex (LMMs: sex: $F(1,171) = 0.600$, $p = 0.439$, Hedges's $g = 0.1477$). However, the interaction between sex and exposure was significant (LMMs: sex*exposure: $F(1,171) = 8.417$, $p = 0.004$). In order to further evaluate the possible differences in males and females groups, LMMs was performed and revealed that exposure did not modulate the NMDA sEPSC amplitude between SAC and PAE males (LMMs: exposure: $F(1,27.022) = 1.445$, $p = 0.240$; Hedges's $g = 0.3752$). The random effect of litter significantly improved LMM and was included in the final model. On the other hand, PAE females showed a significant increase of amplitude compared to SAC controls (LMMs: exposure: $F(1,84) = 5.449$, $p = 0.022$; Hedges's $g = 0.479$). (Fig 1C). During the building of this LMM, the random effect of litter did not significantly improve the model and subsequently it was removed from the final LMM.

LMM analysis of the current density revealed a significant sex*exposure interaction (LMMs: sex*exposure: $F(1,177) = 6.952$, $p = 0.009$), but not effect of sex or exposure (LMMs: sex: $F(1,177) = 0.001$, $p = 0.978$, Hedges's $g = 0.0271$; exposure: $F(1,177) = 0.026$, $p = 0.873$, Hedges's $g = 0.018$). Since, the statistical analysis indicated a sex*exposure effect, the LMMs within sex indicated that exposure to EtOH induces a significant decrease of current density in PAE males (LMMs: exposure: $F(1,87) = 4.262$, $p = 0.042$; Hedges's $g = 0.4334$). While, in females the statistical analysis did not reveal a significant effect (LMMs: exposure: $F(1,90) = 2.847$, $p = 0.095$, Hedges's $g = 0.3528$ (Fig 1D). For all three models, the random effect of litter was not included in final LMMs, because likelihood ratio testing indicated it did not significantly improve the model.

The decay time of NMDA eEPSC was not modulated by PAE in all experimental groups (LMMs: sex: $F(1,132.545) = 0.673$, $p = 0.414$, Hedges's $g = 0.0193$; sex*exposure effect: $F(1, 132.545) = 0.065$, $p = 0.800$; exposure: $F(1,36.981) = 0.037$, $p = 0.849$, Hedges's $g = 0.0145$) (Fig 1E). In the present LMM, the random effect of litter was included in the final model, since the p-value of likelihood ratio test was < 0.05.

Consistent with results of decay kinetics, the total charge transfer of NMDA-eEPSCs (measured calculating the area under the curve) was not significantly affected by PAE (LMMs: exposure: $F(1,173) = 0.302$, $p = 0.583$, Hedges's $g = 0.0785$). LMM also found no significant effect of sex or sex*exposure interaction (LMM: sex: $F(1,173) = 0.012$, $p = 0.914$, Hedges's $g = 0.278$; sex*exposure effect: $F(1,173) = 2.247$, $p = 0.136$) (Fig 1F). The p-value of likelihood ratio test in the present model was > 0.05, and therefore random effect of litter was excluded from the final model.

PAE does not affect NMDA/GluN2B mediated currents

To determine the PAE effects on NMDA-eEPSCs mediated by receptors containing the GluN2B subunit, eEPSCs were recorded in presence of Ro25–6981 (1 μM). The selective antagonist was bath-applied for 15 minutes (Fig 2A, 2B). We calculated the effect of drug considering the last 5 minutes of perfusion, the statistical analysis performed on amplitude does not reveal a significant difference in all experimental groups (LMMs: sex: $F_{(1,86)} = 0.174$, $p = 0.678$, Hedges's g = 0.076; exposure $F_{(1,86)} = 0.798$, $p = 0.374$, Hedges's g = 0.1561; sex*exposure effect: $F_{(1,86)} = 1668$, $p = 0.200$) (Fig. 2C). Also, the application of Ro25–6981 did not modulate the decay time of eEPSCs (LMMs: sex: $F_{(1,74)} = 1.286$, $p = 0.260$, Hedges's g = 0.296; exposure: $F_{(1,74)} = 1.151$, $p = 0.287$, Hedges's g = 0.2844; sex*exposure effect: $F_{(1,74)} = 1.835$, $p = 0.180$) (Fig. 2D). In both final LMMs, the random effect of litter was excluded from the final model because it did not improve significantly the models.

Comparing the total charge transfer of NMDA-eEPSCs calculated before and after Ro25–6981 bath-application, the LMM did not find a significant effect (LMMs: sex: $F_{(1,86)} = 0.364$, $p = 0.548$, Hedges's g = 0.076; exposure: $F_{(1,86)} = 0.096$, $p = 0.757$, Hedges's g = 0.1561; sex*exposure effect: $F_{(1,86)} = 0.315$, $p = 0.576$) (Fig. 2F). The litter random effect was not included as it did not improve the final model (likelihood ratio test p-value > 0.05).

PAE does not significantly alter the synaptic NMDAR subunits GluN1 and GluN2B expression

We quantified the NMDAR subunits GluN1 and GluN2B protein levels specifically in the synaptic membrane fraction bound to the post-synaptic density using immunoblotting (Fig 3A–D). There were no significant differences in the GluN1 subunit expression between SAC and PAE treatment (Two-way ANOVA: exposure: $F_{(1,16)} = 0.061833$, $p = 0.8068$) or due to sex (Two-way ANOVA: sex: $F_{(1,16)} = 0.2154$, $p = 0.6488$). Moreover, the analysis revealed no significant sex*exposure effect (Two-way ANOVA: sex*exposure: $F_{(1,16)}=0.1793$, $p = 0.6676$) (Fig.3A). With regards to the GluN2B subunit expression we found no significant difference after PAE (Two-way ANOVA: exposure: $F_{(1,8)} = 0.2750$, $p = 0.6142$) in both sexes (Two-way ANOVA: sex: $F_{(1,8)} = 2.019$, $p = 0.1931$), and also no significant sex*exposure interaction (Two-way ANOVA: sex*exposure: $F_{(1,8)}=0.8061$, $p = 0.3955$) (Fig.3B). We further looked at the ratio of GluN2B/GluN1, which again revealed that PAE does not modulate the GluN2B subunit expression in all experimental groups (Two-way ANOVA: exposure: $F_{(1,8)} = 0.3532$, $p = 0.5687$: sex: $F_{(1,8)} = 1.462$, $p = 0.2611$; sex*exposure: $F_{(1,8)} = 1.368$, $p = 0.2758$) (Fig.3C).

Discussion

We have previously shown that moderate PAE is sufficient to impair cognitive function and alter the firing and coordination of OFC pyramidal neurons in mice (Marquardt et al., 2014), and that these alterations are accompanied by changes in both cortical and striatal firing and coordination (Marquardt et al., 2020). To investigate a molecular mechanism through which PAE may impair behavioral flexibility, we characterized the evoked currents mediated by NMDARs in OFC pyramidal neurons from offspring of alcohol-exposed dams. Analysis

of different passive electrical properties revealed that a low level of PAE did not alter the membrane cell capacitance in either sex, although the membrane resistance was altered in a sex specific manner. Females, on average, had a lower membrane resistance compared to males, suggesting that cells from females may have higher membrane conductance. Measuring NMDA-eEPSCs, we also found a significant interaction effect of sex and exposure on current amplitude. Further analysis showed that PAE females had a significantly larger amplitude compared to control females. A significant interaction effect of sex and exposure was also seen on current density that differed from amplitude, as male PAE mice had a significant decrease compared to SAC male. These data suggest that PAE may modulate synaptic NMDA-eEPSCs in a sex-specific manner.

Our current findings add weight to previous work showing that PAE may lead to sex x stress specific changes in other brain regions such as reduced NMDAR-dependent long term potentiation (LTP) in dentate gyrus (DG) in adolescent male, but not in female rats (Titterness and Christie, 2012). Similar results were also found in hippocampal LTP in adult male, but not in female PAE offspring (Sickmann et al., 2014). To our knowledge, these findings are the first to show PAE sex specific effects on NMDAR function in OFC pyramidal neurons. While it is not clear why PAE may alter the NMDA-eEPSCs amplitude and current density differentially in females and males, we have to consider the pattern of increasing current density in PAE females indicating an enhanced NMDA functionality. Our results suggest that PAE may induce neurophysiological adaptations during cortical development associated with an increase in number and function of NMDARs in females, and a decrease in males. Interestingly, it was reported that glutamine synthetase expression in DG was increased after PAE consistent with altered excitatory neurotransmission in exposed animals (Sickmann et al., 2014).

Surprisingly, the pharmacological isolation of NMDA-eEPSCs mediated by GluN2B subunit in the current study did not reveal any significant effect mediated by PAE in OFC pyramidal neurons. These data are in contrast with a previous study showing that PAE significantly enhanced NMDA-eEPSCs mediated by GluN2B subunit in agranular insular cortex (AIC) (Bird et al. 2015). These discrepancies could be due to multiple factors including the different brain regions examined (AIC vs. OFC), and the different GluN2B antagonist used (ifenprodil vs. Ro25–6981). However, immunoblotting results performed using OFC total synaptic fraction are consistent with ex-vivo recording, in fact GluN2B expression was not significantly altered by PAE. We found that protein levels measured in OFC from PAE male mice were lower than control, and eEPSCs-amplitude mediated by GluN2B was increased. Although neither difference was significant, these results may be consistent with findings showing that PAE modulates the NMDA-EPSCs amplitude and with significant reduction of GluN2B expression measured in the dentate gyrus of the hippocampus after prenatal treatment (Brady et al., 2013).

One possible mediator of the interaction of PAE and sex may be stress responsivity. The PAE model used in the current study has previously been shown to significantly alter the hypothalamic pituitary adrenal (HPA) axis in offspring (Caldwell et al., 2014; Caldwell et al., 2015). Stress exposure itself during gestation has been shown to affect brain development and induce cognitive impairments (Fumagalli et al., 2009). Together with data

showing that PAE offspring, and specifically PAE females, are hyper-responsive to stressors in adulthood (Weinberg, 1989). PAE itself may act as a stressor that differentially affects males and females during gestation altering later stress responses and cognition across the lifespan. However, future studies are required to examine in detail how PAE induces and modulates stress response across sexes.

Another possible factor regarding sex x treatment interaction is estrous cycle, as it has previously been shown that it modulates neuronal electrophysiological properties in different brain regions. Specifically, passive membrane properties, action potential threshold and firing rate differ by cycle-state in rat caudate-putamen medium spiny neurons (Willett et al., 2020). It has been demonstrated that cortical fast spiking interneurons are cyclically regulated by the estrous phase indicating that sex hormones modulate cortical inhibition in females (Clemens et al., 2019). In the current study, female PAE and SAC mice were entrained, but we did not identify the specific estrous cycle phases in each mouse prior to the whole-cell recordings. Future studies are required to examine whether differences in PAE females are specific to estrous phase.

Dose and timing of exposure are also well established to impact the behavioural effects of PAE in offspring and may explain difference in the reported alterations on NMDAR subunit expression. Here, we used behavioural naive offspring from dams having a low average EtOH consumption (3.91 ± 0.18 g/kg/day) compared with those of previous studies that had almost double the daily intake (Brady et al., 2013; 6.9 g/kg/day). Timing is also critical, as a single day of ethanol exposure during gestation was found to modulate GluN2B, as well as GluN2A subunits expression differently during the embryonic development and adulthood (Toso et al., 2005). Specifically, brains of adult mice exposed prenatally to alcohol showed a significant downregulation in GluN2B expression and subsequent upregulation in GluN2A protein levels (Toso et al., 2005). Localization is also an important variable, and the role of subunits in both synaptic and extra-synaptic NMDAR needs to be better understood. This is particularly important considering that GluN2B subunits have been reported to be mainly localized in extra-synaptic NMDARs, while GluN2A subunits are expressed in synaptic sites (Petralia, 2012). In addition, analysis of eEPSC decay kinetics and total charge transfer showed no significant differences between SAC and PAE offspring compared to the significant alteration in amplitude. This further supports the possible involvement of other NMDAR subunits, given differences in decay kinetics between GluN2A and GluN2B diheteromeric NMDAR (Vicini et al., 1998). Given these findings, further studies are required to understand the dose required to alter NMDAR function in offspring, as well as the role that GluN2A modulation play in both functional and behavioural outcome in PAE offspring.

Taken together, our findings indicate that PAE alters NMDA receptor activity in OFC in a sex-dependent manner. We observed a significant positive modulation of NMDA-eEPSCs amplitude in PAE females, and a reduction in current density in PAE males. Future investigations will be required to examine the eEPSCs mediated by different NMDA subunits at different ages, and characterize possible neuro-adaptations induced by PAE in the cortex. Overall, these findings show that even low levels of alcohol exposure during

gestation can lead to long lasting sex-specific changes in cortical NMDAR function, which may mediate the reversal learning deficits seen in mouse models of FASD.

Acknowledgements

References:

Anson LC, Chen PE, Wyllie DJ, Colquhoun D, Schoepfer R (1998) Identification of amino acid residues of the NR2A subunit that control glutamate potency in recombinant NR1/NR2A NMDA receptors. J Neurosci 18:581–589. [PubMed: 9425000]

Brady ML, Allan AM, Caldwell KK (2012) A limited access mouse model of prenatal alcohol exposure that produces long-lasting deficits in hippocampal-dependent learning and memory. Alcohol Clin Exp Res 36:457–466. [PubMed: 21933200]

Brady ML, Diaz MR, Iuso A, Everett JC, Valenzuela CF, Caldwell KK (2013) Moderate prenatal alcohol exposure reduces plasticity and alters NMDA receptor subunit composition in the dentate gyrus. J Neurosci 33:1062–1067. [PubMed: 23325244]

Brigman JL, Daut RA, Wright T, Gunduz-Cinar O, Graybeal C, Davis MI, Jiang Z, Saksida LM, Jinde S, Pease M, Bussey TJ, Lovinger DM, Nakazawa K, Holmes A (2013) GluN2B in corticostriatal circuits governs choice learning and choice shifting. Nat Neurosci 16:1101–1110. [PubMed: 23831965]

Burden MJ, Jacobson SW, Jacobson JL (2005a) Relation of prenatal alcohol exposure to cognitive processing speed and efficiency in childhood. Alcohol Clin Exp Res 29:1473–1483. [PubMed: 16131856]

Burden MJ, Jacobson SW, Sokol RJ, Jacobson JL (2005b) Effects of prenatal alcohol exposure on attention and working memory at 7.5 years of age. Alcohol Clin Exp Res 29:443–452. [PubMed: 15770121]

Caldwell KK, Goggin SL, Tyler CR, Allan AM (2014) Prenatal alcohol exposure is associated with altered subcellular distribution of glucocorticoid and mineralocorticoid receptors in the adolescent mouse hippocampal formation. Alcohol Clin Exp Res 38:392–400. [PubMed: 23992407]

Caldwell KK, Goggin SL, Labrecque MT, Allan AM (2015) The impact of prenatal alcohol exposure on hippocampal-dependent outcome measures is influenced by prenatal and early-life rearing conditions. Alcohol Clin Exp Res 39:631–639. [PubMed: 25752869]

Carpenter-Hyland EP, Woodward JJ, Chandler LJ (2004) Chronic ethanol induces synaptic but not extrasynaptic targeting of NMDA receptors. J Neurosci 24:7859–7868. [PubMed: 15356198]

Clark E, Antoniak K, Feniquito A, Dringenberg HC (2017) Effects of the GluN2B-NMDA receptor antagonist Ro 25–6981 on two types of behavioral flexibility in rats. Behav Brain Res 319:225–233. [PubMed: 27871866]

Clemens AM, Lenschow C, Beed P, Li L, Sammons R, Naumann RK, Wang H, Schmitz D, Brecht M (2019) Estrus-Cycle Regulation of Cortical Inhibition. Curr Biol 29:605–615.e606. [PubMed: 30744972]

Cull-Candy S, Brickley S, Farrant M (2001) NMDA receptor subunits: diversity, development and disease. Curr Opin Neurobiol 11:327–335. [PubMed: 11399431]

Day NL, Helsel A, Sonon K, Goldschmidt L (2013) The association between prenatal alcohol exposure and behavior at 22 years of age. Alcohol Clin Exp Res 37:1171–1178. [PubMed: 23442183]

Dong Z, Bai Y, Wu X, Li H, Gong B, Howland JG, Huang Y, He W, Li T, Wang YT (2013) Hippocampal long-term depression mediates spatial reversal learning in the Morris water maze. Neuropharmacology 64:65–73. [PubMed: 22732443]

Ehrhart F, Roozen S, Verbeek J, Koek G, Kok G, van Kranen H, Evelo CT, Curfs LMG (2019) Review and gap analysis: molecular pathways leading to fetal alcohol spectrum disorders. Mol Psychiatry 24:10–17. [PubMed: 29892052]

Fontaine CJ, Patten AR, Sickmann HM, Helfer JL, Christie BR (2016) Effects of pre-natal alcohol exposure on hippocampal synaptic plasticity: Sex, age and methodological considerations. Neurosci Biobehav Rev 64:12–34. [PubMed: 26906760]

Fumagalli F, Pasini M, Frasca A, Drago F, Racagni G, Riva MA (2009) Prenatal stress alters glutamatergic system responsiveness in adult rat prefrontal cortex. J Neurochem 109:1733–1744. [PubMed: 19383086]

Goebel-Goody SM, Davies KD, Alvestad Linger RM, Freund RK, Browning MD (2009) Phospho-regulation of synaptic and extrasynaptic N-methyl-d-aspartate receptors in adult hippocampal slices. Neuroscience 158:1446–1459. [PubMed: 19041929]

Golub MS, Sobin CA (2020) Statistical modeling with litter as a random effect in mixed models to manage "intralitter likeness". Neurotoxicol Teratol 77:106841. [PubMed: 31863841]

Kenton JA, Ontiveros T, Bird CW, Valenzuela CF, Brigman JL (2020) Moderate prenatal alcohol exposure alters the number and function of GABAergic interneurons in the murine orbitofrontal cortex. Alcohol 88:33–41. [PubMed: 32540413]

Lange S, Probst C, Gmel G, Rehm J, Burd L, Popova S (2017) Global Prevalence of Fetal Alcohol Spectrum Disorder Among Children and Youth: A Systematic Review and Meta-analysis. JAMA Pediatr 171:948–956. [PubMed: 28828483]

Laube B, Hirai H, Sturgess M, Betz H, Kuhse J (1997) Molecular determinants of agonist discrimination by NMDA receptor subunits: analysis of the glutamate binding site on the NR2B subunit. Neuron 18:493–503. [PubMed: 9115742]

Lynch ME, Kable JA, Coles CD (2015) Prenatal alcohol exposure, adaptive function, and entry into adult roles in a prospective study of young adults. Neurotoxicol Teratol 51:52–60. [PubMed: 26247662]

Mårdby AC, Lupattelli A, Hensing G, Nordeng H (2017) Consumption of alcohol during pregnancy-A multinational European study. Women Birth 30:e207–e213. [PubMed: 28111037]

Marquardt K, Cavanagh JF, Brigman JL (2020) Alcohol exposure in utero disrupts cortico-striatal coordination required for behavioral flexibility. Neuropharmacology 162:107832. [PubMed: 31678398]

Marquardt K, Sigdel R, Caldwell K, Brigman JL (2014) Prenatal ethanol exposure impairs executive function in mice into adulthood. Alcohol Clin Exp Res 38:2962–2968. [PubMed: 25581651]

Marquardt K, Josey M, Kenton JA, Cavanagh JF, Holmes A, Brigman JL (2019) Impaired cognitive flexibility following NMDAR-GluN2B deletion is associated with altered orbitofrontal-striatal function. Neuroscience 404:338–352. [PubMed: 30742964]

May PA, Gossage JP, Kalberg WO, Robinson LK, Buckley D, Manning M, Hoyme HE (2009) Prevalence and epidemiologic characteristics of FASD from various research methods with an emphasis on recent in-school studies. Dev Disabil Res Rev 15:176–192. [PubMed: 19731384]

May PA, Baete A, Russo J, Elliott AJ, Blankenship J, Kalberg WO, Buckley D, Brooks M, Hasken J, Abdul-Rahman O, Adam MP, Robinson LK, Manning M, Hoyme HE (2014) Prevalence and characteristics of fetal alcohol spectrum disorders. Pediatrics 134:855–866. [PubMed: 25349310]

Olney JW (2004) Fetal alcohol syndrome at the cellular level. Addict Biol 9:137–149; discussion 151. [PubMed: 15223539]

Paoletti P (2011) Molecular basis of NMDA receptor functional diversity. Eur J Neurosci 33:1351–1365. [PubMed: 21395862]

Paoletti P, Bellone C, Zhou Q (2013) NMDA receptor subunit diversity: impact on receptor properties, synaptic plasticity and disease. Nat Rev Neurosci 14:383–400. [PubMed: 23686171]

Petralia RS (2012) Distribution of extrasynaptic NMDA receptors on neurons. ScientificWorldJournal 2012:267120. [PubMed: 22654580]

Pfinder M, Lhachimi S (2020) Lifestyle-related risk factors during pregnancy: even low-to-moderate drinking during pregnancy increases the risk for adolescent behavioral problems. Journal of Substance Use 25:135–140.

Popova S, Lange S, Probst C, Gmel G, Rehm J (2017) Estimation of national, regional, and global prevalence of alcohol use during pregnancy and fetal alcohol syndrome: a systematic review and meta-analysis. Lancet Glob Health 5:e290–e299. [PubMed: 28089487]

Saito M, Mao RF, Wang R, Vadasz C, Saito M (2007) Effects of gangliosides on ethanol-induced neurodegeneration in the developing mouse brain. Alcohol Clin Exp Res 31:665–674. [PubMed: 17374046]

Samudio-Ruiz SL, Allan AM, Sheema S, Caldwell KK (2010) Hippocampal N-methyl-D-aspartate receptor subunit expression profiles in a mouse model of prenatal alcohol exposure. Alcohol Clin Exp Res 34:342–353. [PubMed: 19951292]

Shipton OA, Paulsen O (2014) GluN2A and GluN2B subunit-containing NMDA receptors in hippocampal plasticity. Philos Trans R Soc Lond B Biol Sci 369:20130163.

Sickmann HM, Patten AR, Morch K, Sawchuk S, Zhang C, Parton R, Szlavik L, Christie BR (2014) Prenatal ethanol exposure has sex-specific effects on hippocampal long-term potentiation. Hippocampus 24:54–64. [PubMed: 23996604]

Skorput AG, Yeh HH (2016) Chronic Gestational Exposure to Ethanol Leads to Enduring Aberrances in Cortical Form and Function in the Medial Prefrontal Cortex. Alcohol Clin Exp Res 40:1479–1488. [PubMed: 27242215]

Tan CH, Denny CH, Cheal NE, Sniezek JE, Kanny D (2015) Alcohol use and binge drinking among women of childbearing age - United States, 2011–2013. MMWR Morb Mortal Wkly Rep 64:1042–1046. [PubMed: 26401713]

Thomas JD, Garcia GG, Dominguez HD, Riley EP (2004) Administration of eliprodil during ethanol withdrawal in the neonatal rat attenuates ethanol-induced learning deficits. Psychopharmacology (Berl) 175:189–195. [PubMed: 15064913]

Titterness AK, Christie BR (2012) Prenatal ethanol exposure enhances NMDAR-dependent long-term potentiation in the adolescent female dentate gyrus. Hippocampus 22:69–81. [PubMed: 21080406]

Toso L, Poggi SH, Abebe D, Roberson R, Dunlap V, Park J, Spong CY (2005) N-methyl-D-aspartate subunit expression during mouse development altered by in utero alcohol exposure. Am J Obstet Gynecol 193:1534–1539. [PubMed: 16202752]

Vicini S, Wang JF, Li JH, Zhu WJ, Wang YH, Luo JH, Wolfe BB, Grayson DR (1998) Functional and pharmacological differences between recombinant N-methyl-D-aspartate receptors. J Neurophysiol 79:555–566. [PubMed: 9463421]

Weinberg J (1989) Prenatal ethanol exposure alters adrenocortical development of offspring. Alcohol Clin Exp Res 13:73–83. [PubMed: 2538092]

West BT, Welch KB, Galecki AT (2007) Linear mixed models : a practical guide using statistical software. Boca Raton: Chapman & Hall/CRC.

Willett JA, Cao J, Johnson A, Patel OH, Dorris DM, Meitzen J (2020) The estrous cycle modulates rat caudate-putamen medium spiny neuron physiology. Eur J Neurosci 52:2737–2755. [PubMed: 31278786]

Wilson SE, Cudd TA (2011) Focus on: the use of animal models for the study of fetal alcohol spectrum disorders. Alcohol Res Health 34:92–98. [PubMed: 23580046]
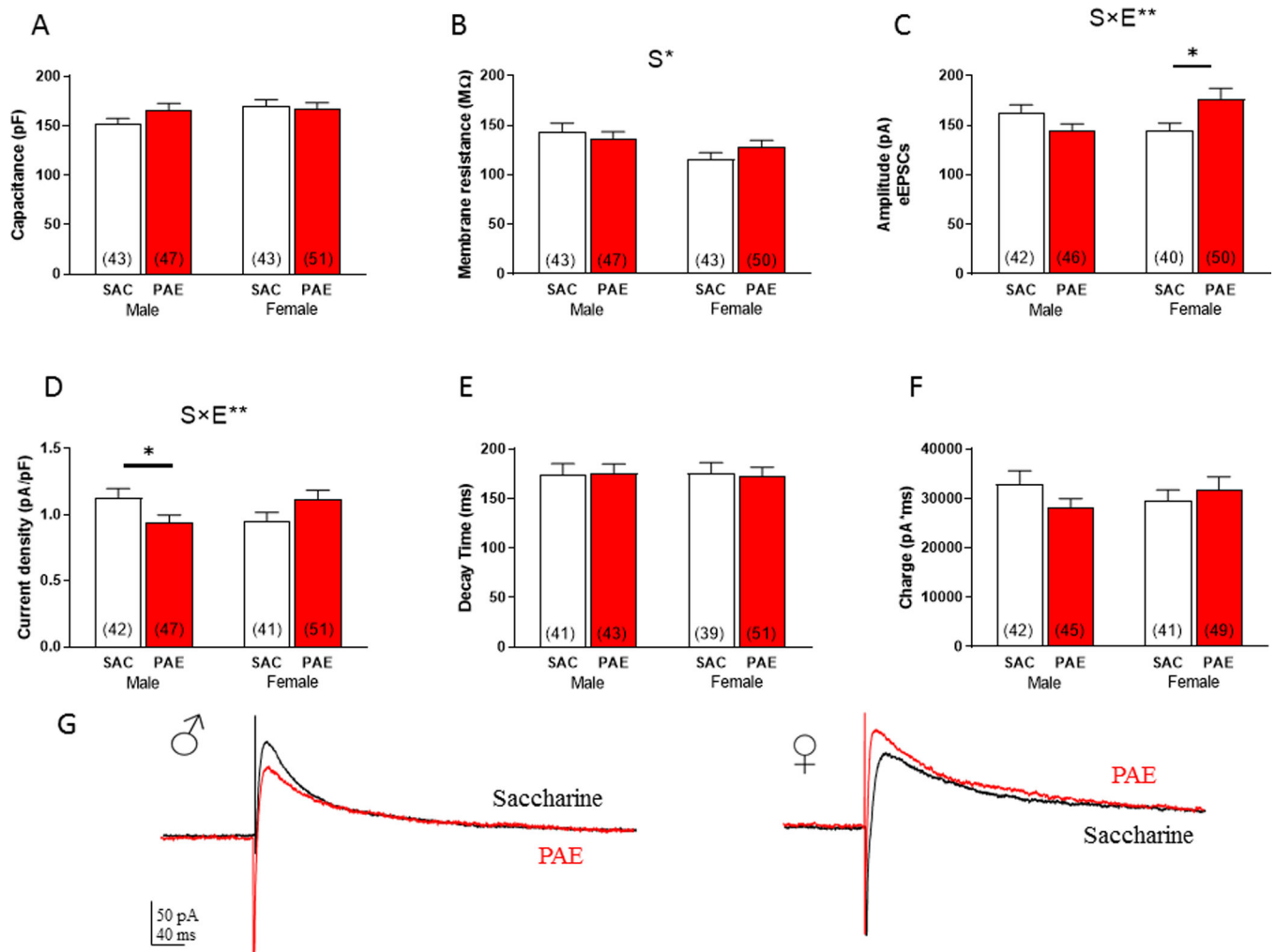
Figure 1. Effects of prenatal alcohol exposure on evoked NMDA currents (eEPSCs) in orbital frontal cortex (OFC) pyramidal neurons.
A. Prenatal alcohol treatment does not alter the capacitance of OFC pyramidal neurons from SAC and PAE animals. **B.** Bar graphs reporting the sex effect (S) on membrane resistance. **C.** Treatment induces a significant sex*exposure (S*E) effect for NMDA-eEPSCs amplitude, and PAE females show a significant increase of eEPSCs amplitude. **D.** Current density shows a significant S*E effect, and a significant decrease in PAE males compared SAC males. **E.** Decay time results to be not affected by treatment in all experimental groups. **F.** Bar graphs showing the total charge transfer of eEPSCs. **G.** Representative traces of evoked NMDA currents. Data are presented as mean ± SEM. The number of cells included in the analysis is shown in parenthesis. $p < 0.05$, ** $p < 0.01$.
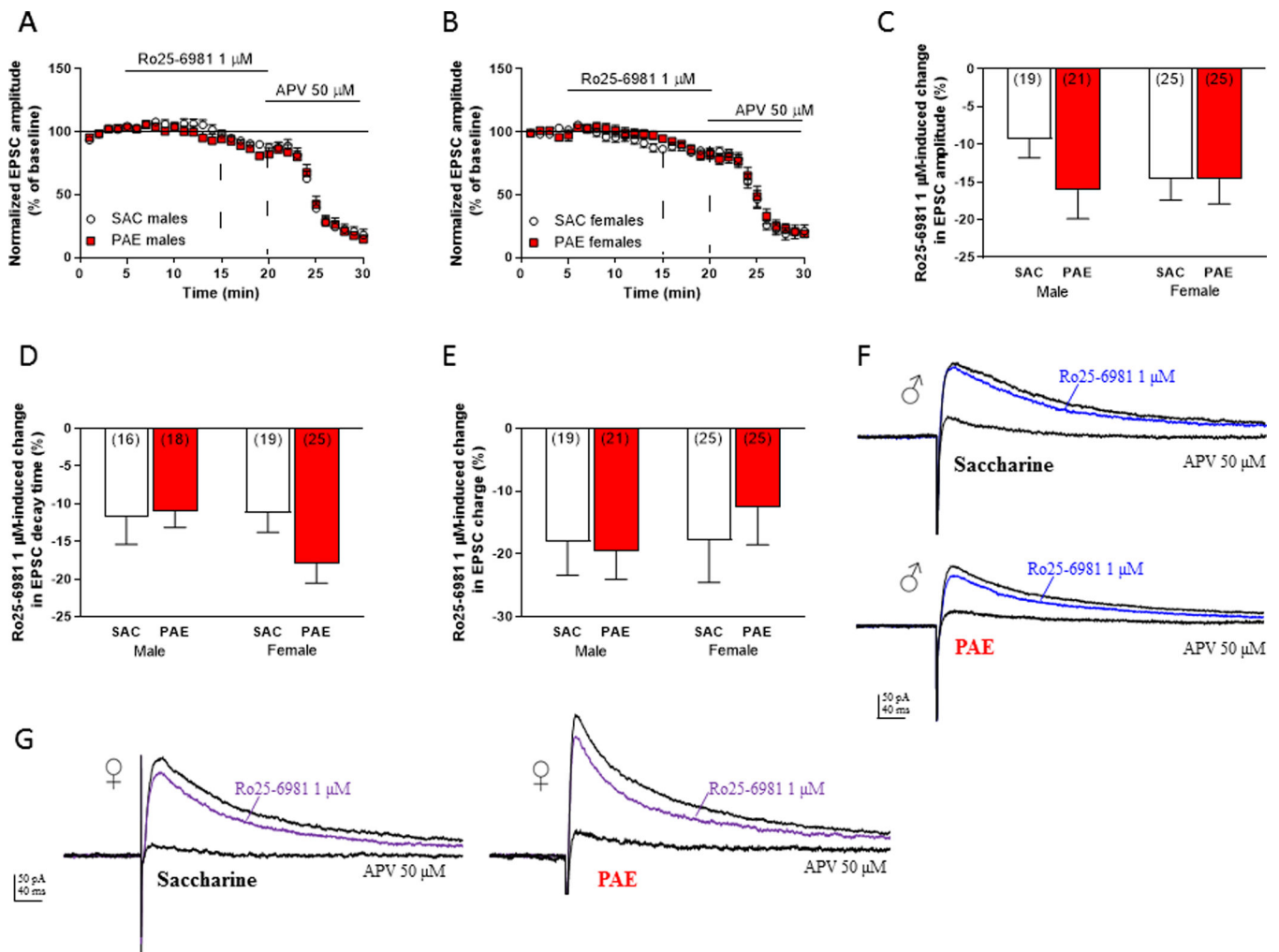
Figure 2. Pharmacological isolation of evoked NMDA eEPSCs mediated by GluN2B subunit.
A–B. Time course plots showing the NMDA eEPSCs amplitude before, during Ro25–
6981 and APV bath-application in slices coming from SAC and PAE males and females
respectively. **C.** Bar graphs reporting the effect of Ro25–6981 antagonism on eEPSCs-
amplitude indicated as a percentage change from baseline calculated during the last 5
minutes of drug bath-perfusion (indicated with dashed line rectangle in Fig 2.A, B). **D**.
Ro25–6981 does not alter the decay time of the NMDA eEPSCs (effect calculated in the
last 5 minutes of drug bath-perfusion and indicated as a percentage change from baseline) in
all experimental groups. **E.** Total Charge of NMDA eEPSCs mediated by GluN2B subunit
is not modulated by PAE in male and female mice (reported as percentage change from
baseline calculated considering the last 5 minutes of Ro25–6981 bath-application). **F–G.**
Representative traces showing the effect of Ro25–6981 antagonist on NMDA eEPSCs
mediated in female groups. Data are presented as mean ± SEM. The number of cells
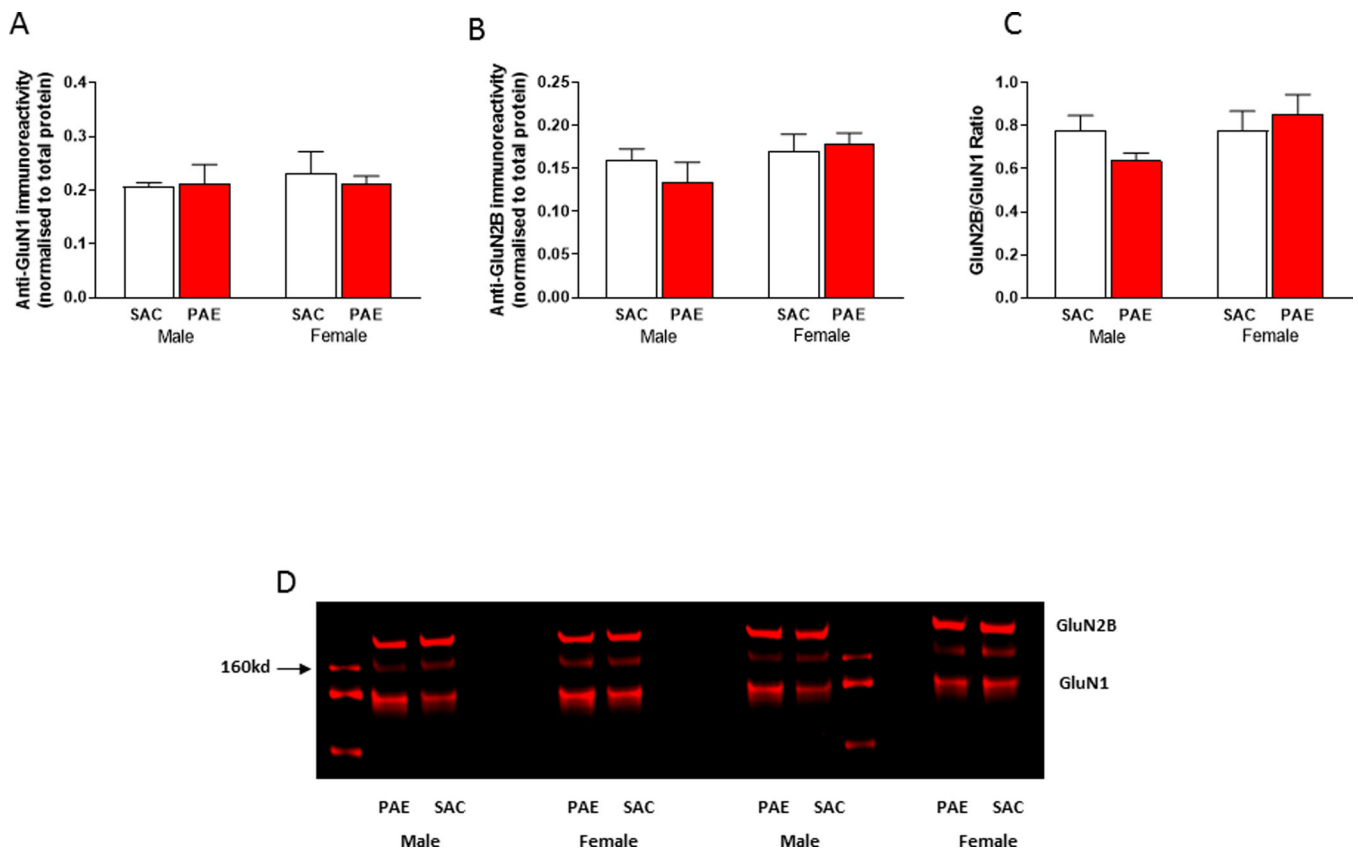included in the analysis is shown in parenthesis.

Figure 3: Moderate prenatal alcohol exposure did not significantly alter the NMDAR subunit expression in the synaptic fraction of OFC.

A. No significant difference in GluN1 subunit expression of the NMDAR between SAC and PAE. n=5/group (20 mice/group, 4 mice pooled /group) **B.** No significant difference in GluN2B subunit expression of the NMDAR between SAC and PAE. n=5/group (20 mice/group, 4 mice pooled /group) **C.** The ratio of GluN2B/GluN1 revealed no significant difference between SAC and PAE in both male and female mice. n=5 /group 20 mice/group, 4 mice pooled /group) **D.** Representative image of GluN2B, GluN1 expression. Data are presented as mean ± SEM.

Table 1.

Characteristic of NMDA-eEPSCs.

Average of measured values for capacitance, membrane resistance, amplitude, current density, decay time and total charge transfer of NMDA-eEPSCs are reported as mean ± SEM. The effect of Ro25–6981 on amplitude, total charge transfer and decay time is reported as mean (SEM) % reduction.

	SAC Males	PAE Males	SAC Females	PAE Females
Capacitance (pF)	152 ± 5.146	166.3 ± 6.257	169.7 ± 6.797	166.8 ± 6.209
Membrane Resistance (MΩ)	143.1 ± 9.017	136.0 ± 7.429	115.7 ± 6.501	128 ± 6.647
Amplitude (pA)	162.8 ± 7.636	143.9 ± 7.480	144.2 ± 7.838	176.1 ± 11.12
Current Density (pA/pF)	1.127 ± 0.070	0.936 ± 0.060	0.945 ± 0.070	1.114 ± 0.069
Decay Time (ms)	174.1 ± 11.13	175.5 ± 9.521	175.2 ± 11.06	172.2 ± 9.425
Charge (pA*ms)	32895 ± 2730	28086 ± 1881	29631 ± 2101	31859 ± 2517
Amplitude after Ro25–6981 (% of variation vs baseline)	−9.37 ± 2.489	−16.09 ± 2.489	−14.59 ± 2.846	−14.63 ± 3.266
Decay Time after Ro25–6981 (% of variation vs baseline)	−11.80 ± 3.585	−11.02 ± 2.149	−11.19 ± 2.588	−17.93 ± 2.603
Charge after Ro25–6981 (% of variation vs baseline)	−18.03 ± 5.369	−19.52 ± 4.529	−17.78 ± 6.772	−12.61 ± 5.936

Table 2.

Linear Mixed-Model Analysis.

Linear Mixed-Models are built indicating if random effect of litter or heterogeneous error variances for each variable significantly improved the model. F-ratios and p-values are reported for sex, exposure effects and interaction between these effects. Hedges's g effect size is reported for sex and exposure effects. Mann-Whitney U tests(effect size is included as r) are reported for both fixed effects from LMMs with residuals that violate assumption of normality (Shapiro-Wilk test).

Fig.	Variable	Random effect of litter	Heterogeneous or Homogenoeus	Sex	Exposure	Sex*Exposure	Passes SW normality test?	Mann-Whitney U:Sex	Mann-Whitney U:Exposure
1A	Capacitance	No	Homogeneous	$F_{(1,180)}=2.127$ p=0.147 g=0.2042	$F_{(1,180)}=0.831$ p=0.363 g=0.1342	$F_{(1,180)}=1.876$ p=0.172	No	U(n1=94,n2=90)=3800 p=0.234 r=0.087	U(n1=98,n2=86)=3900 p=0.384 r=0.064
1B	**Membrane Resistance**	No	Homogeneous	**$F_{(1,179)}=5.662$ p=0.018 g=0.3383**	$F_{(1,179)}=0.119$ p=0.730 g=0.0478	$F_{(1,179)}=1.713$ p=0.192	No	U(n1=93,n2=90)=3435 p=0.036 r=0.154	U(n1=97,n2=86)=4051 p=0.738 r=0.024
1C	**Amplitude Baseline**	No	Heterogeneous	$F_{(1,171)}=0.600$ p=0.439 g=0.1477	$F_{(1,171)}=0.535$ p=0.466 g=0.1136	**$F_{(1,171)}=8.417$ p=0.004**	No	U(n1=90,n2=88)=3801 p=0.644 r=0.034	U(n1=96,n2=82)=3919 p=0.960 r=0.003
1C	**Amplitude Female**	No	Heterogeneous	-	**$F_{(1,84)}=5.449$ p=0.022 g=0.479**	-	No	-	U(n1=50,n2=40)=786 p=0.082 r=0.183
1C	Amplitude Male	Yes	Homogeneous	-	$F_{(1,27.022)}=1.445$ p=0.240 g=0.3752	-	No	-	U(n1=46,n2=42)=746 p=0.066 r=0.195
1D	**Current density**	No	Homogeneous	$F_{(1,177)}=0.001$ p=0.978 g=0.0271	$F_{(1,177)}=0.026$ p=0.873 g=0.018	**$F_{(1,177)}=6.952$ p=0.009**	No	U(n1=92,n2=89)=4052 p=0.905 r=0.008	U(n1=98,n2=83)=3959 p=0.758 r=0.022
1D	Current density Female	No	Homogeneous	-	$F_{(1,90)}=2.847$ p=0.095 g=0.3528	-	No	-	U(n1=51,n2=41)=827 p=0.086 r=0.178
1D	**Current density Male**	No	Homogeneous	-	**$F_{(1,87)}=4.262$ p=0.042 g=0.4334**	-	No	-	U(n1=47,n2=42)=699 p=0.018 r=0.2509
1E	Decay Time Baseline	Yes	Homogeneous	$F_{(1,132.545)}=0.673$ p=0.414 g=0.0193	$F_{(1,36.981)}=0.037$ p=0.849 g=0.0145	$F_{(1,132.545)}=0.065$ p=0.800	No	U(n1=90,n2=84)=3729 p=0.878 r=0.011	U(n1=94,n2=80)=3739 p=0.949 r=0.004

Fig.	Variable	Random effect of litter	Heterogeneous or Homogenoeus	Sex	Exposure	Sex*Exposure	Passes SW normality test?	Mann-Whitney U:Sex	Mann-Whitney U:Exposure
1F	Charge Baseline	No	Homogeneous	F(1,173)=0.012 p=0.914 g=0.278	F(1,173)=0.302 p=0.583 g=0.0785	F(1,173)=2.247 p=0.136	No	U(n1=90,n2=87)=3835 p=0.816 r=0.0175	U(n1=94,n2=83)=3609,5 p=0.392 r=0.0644
2C	Amplitude after Ro25–6981	No	Homogeneous	F(1,86)=0.174 p=0.678 g=0.076	F(1,86)=0.798 p=0.374 g=0.1561	F(1,86)=1.668 p=0.200	Yes		
2D	Decay Time after Ro25–6981	No	Homogeneous	F(1,74)=1.286 p=0.260 g=0.296	F(1,74)=1.151 p=0.287 g=0.2884	F(1,74)=1.835 p=0.180	Yes	-	-
2E	Charge after Ro25–6981	No	Homogeneous	F(1,86)=0.364 p=0.548 g=0.076	F(1,86)=0.096 p=0.757 g=0.1561	F(1,86)=0.315 p=0.576	No	U(n1=50,n2=40)=984 p=0.897 r=0.0136	U(n1=46,n2=44)=993 p=0.878 r=0.0161